J. Membrane Biol. 177, 81–93 (2000)
DOI: 10.1007/s002320001101

The Journal of
Membrane
Biology

Lithium and Protein Kinase C Modulators Regulate Swelling-Activated K-Cl Cotransport and Reveal a Complete Phosphatidylinositol Cycle in Low K Sheep Erythrocytes

C.M. Ferrell[1], P.K. Lauf[2], B.A. Wilson[3], N.C. Adragna[1]

Departments of Pharmacology and Toxicology[1], Physiology and Biophysics[2], and Biochemistry and Molecular Biology[3], Wright State University, Dayton, Ohio 45435, USA

Received: 1 November 1999/Revised: 6 June 2000

Abstract. K-Cl cotransport (COT), a ouabain-insensitive, Cl-dependent bidirectional K flux, is ubiquitously present in all cells, plays a major role in ion and volume homeostasis, and is activated by cell swelling and a variety of chemical interventions. Lithium modulates several cation transport pathways and inhibits phospholipid turnover in red blood cells (RBCs). Lithium also inhibits K-Cl COT by an unknown mechanism. To test the hypothesis whereby Li inhibits swelling-activated K-Cl COT by altering either its osmotic response, its regulation, or by competing with K for binding sites, low K (LK) sheep (S) RBCs were loaded with Li by Na/Li exchange or the cation ionophore nystatin. K-Cl COT was measured as the Cl-dependent, ouabain-insensitive K efflux or Rb influx. The results show that Li altered the cell morphology, and increased both cell volume and diameter. Internal (Li_i) but not external (Li_o) Li inhibited swelling-activated K-Cl COT by 85% with an apparent K_i of ~7 mM. In Cl, Li_i decreased K efflux at relative cell volumes between 0.9 and 1.2, and at external pHs between 7.2 and 7.4. Li_i reduced the V_{max} and increased the K_m for K efflux in Cl. Furthermore, Li_i increased the production of diacylglycerol in a bimodal fashion, without significant effects on the phosphatidylinositol concentration, and revealed the presence of a complete PI cycle in LK SRBCs. Finally, phorbol ester treatment and PD89059, an inhibitor of mitogen-activated protein kinase (ERK2) kinase, caused a time-dependent inhibition of K-Cl COT. Hence, Li_i appears to inhibit K-Cl COT by acting at an allosteric site on the transporter or its putative regulators, and by modulation of the cellular phospholipid metabolism and a PKC-dependent regulatory pathway, causes an altered response of K-Cl COT to pH and volume.

Key words: Lithium — K-Cl Cotransport — Phosphatidylinositol — Erythrocytes — Protein kinase C — Cell Swelling

Introduction

Red blood cells (RBCs) from various species, including sheep, toadfish, dog, rabbit and man, have been used as models for the study of K-Cl cotransport (COT) and cell volume regulation [13, 21, 23]. K-Cl COT is defined as a Na-independent, Cl-dependent, ouabain-insensitive K flux. In sheep (S) RBCs, this system is stimulated by acid pH, cell swelling, thiol modification, oxidative stress, nitrite (a nitric oxide derivative), Mg depletion and vasodilators [2, 3, 4, 24, 29, 36]). K-Cl COT is inhibited by quinine and quinidine, stilbene derivatives, bumetanide and furosemide [1, 25, 29] and has a low affinity for both of its carried ions. These features distinguish it from other K transport pathways [29].

K-Cl COT is activated by staurosporine and is inhibited by genistein, both kinase inhibitors [8, 15]. In addition, the protein phosphatase 1 (PP1) inhibitors, okadaic acid and calyculin, are inhibitors of the system [19, 22]. The effect of these compounds on K-Cl COT activity suggests control by phosphorylation/dephosphorylation reactions [19]. K-Cl COT is mediated by a ~150 kDa protein with 12 putative transmembrane domains and cytoplasmic N- and C-termini [16]. Of the four isoforms identified, KCC1 is ubiquitously distributed and possesses kinase consensus sites (i.e., phosphorylation by casein kinase and PKC) located on the C-terminal domain [16]. Aside from cytosolic regulation, LK

Correspondence to: N.C. Adragna

SRBC K-Cl COT may be regulated at the membrane level [36, 45] as well as by the L_1 antigen [29].

Alterations in cell morphology have been associated with changes in cell volume during cellular differentiation and pathological conditions such as sickle cell anemia. Nonspherical cells incubated in the presence of Li undergo significant morphological changes [30]. For example, CV1 and HeLa cells become spindlelike and retract from their substrates after several days of Li exposure. Similarly, Li-induced changes in lymphoblastoid and GM1416B cells occur in a concentration- and time-dependent manner. In contrast, HL-60 cells show Li-induced cell surface smoothing and hole development, leading to eventual cell morbidity [51]. Speculations on the mechanism of Li on cell morphology include changes in phospholipid and cholesterol contents, and membrane fluidity. Parker (1986) showed that in dog RBCs, Li decreases the response of K-Cl COT to changes in cell volume and leads to cellular swelling [38, 40].

In skate RBCs, swelling increases the formation of DAG, a PI turnover product and second messenger in the PKC signal transduction pathway [31, 34], suggesting that this pathway may be associated with volume regulation. Furthermore, Li modulates the PI turnover pathway in human RBCs [5]. The complete PI turnover cycle is present in both human and skate RBCs [5, 14, 34] but has not yet been identified in SRBCs.

Li also modulates the transport of other cations (i.e., Ca, Na, K, and H) through competition and allosteric mechanisms [11, 44, 47], and affects kinase and phosphatase activities by displacing Mg from membrane components, ATP and the PI turnover enzyme myo-inositol 1-phosphatase [33, 42, 43].

Here, it is shown that in LK SRBCs, Li_i induced morphological changes and modulated swelling-activated K-Cl COT in a bimodal fashion, inhibiting by a "mixed" noncompetitive mechanism, and in a concentration-dependent manner. Like Li, the PKC modulator, TPA, was found to affect K-Cl COT in a time-dependent bimodal fashion. Agents against specific components of a PKC-dependent signaling pathway, including MAPK and PP-1, were found to inhibit K-Cl COT in LK SRBCs. Li also altered the response of K-Cl COT to pH and cell volume changes. These findings suggest that Li inhibits K-Cl COT by allosteric effects on the cotransporter molecule or via putative regulators. These studies also revealed the presence of a complete PI turnover cycle in LK SRBCs. Thus, Li may affect the response of K-Cl COT to changes in pH and volume through modulation of the cellular phospholipid metabolism and a PKC-dependent pathway.

Materials and Methods

Chemicals

All reagents were of analytical grade. The following chemicals were obtained from Sigma Chemical (St. Louis, MO): LiCl; NaCl; KCl; NaH_2PO_4 and Na_2HPO_4; glucose; sucrose; nystatin; piperazine-N, N′-bis [2-ethanesulfonic acid] (PIPES); N, N-bis [2-hydroxyethyl] glycine (BICINE); N-methyl-D-glucamine (NMDG); 3-[N-morpholino] propane-sulfonic acid (MOPS); 5, 5′-dithiobis-2-nitro-benzoic acid (DTNB); glacial metaphosphoric acid; ethylene diamine tetra-acetic acid (EDTA); 12-o-tetradecanoylphorbol-13-acetate (TPA); calyculin A and Na-citrate; synthetic diolein (C18:1, [cis]-9) of 99% purity, which consisted of two separable isoforms of 1,3-diolein 85% (used for quantitation) and 1,2-cis-diolein 15%; L-alpha-phosphatidylinositol from soybean, 50% purity, which consisted of phosphatidic acid (PA) and phosphatidylethanolamine (PE). TLC plates were Merck Silica gel 60 (H) on glass, 20 × 20 cm and 0.25 mm thick, obtained from Sigma. Chloroform, methanol, petroleum ether and acetic acid were obtained from Fisher Scientific (Pittsburgh, Pa). Iodine crystals were from Matheson Coleman and Bell Manufacturing Chemists (Norwood, OH). PD98059 was purchased from CalBiochem (San Diego, CA).

Blood Collection and Cell Preparation

Blood from a 4–5-year-old Hampshire ewe homozygous for LK RBCs was drawn by jugular venipuncture into heparinized syringes and used within 24 hr or kept overnight in plasma at 4°C. Hb concentration per ml of original packed cells (pc), cellular volume and water content were determined as described previously [12, 20, 24]. Relative cell volume (RCV) was calculated as a ratio of the cell water content of treated cells and that of cells in isosmotic solution. Following buffy coat removal, cells were washed three times with isotonic buffer solution (295 mOsM) containing (mM): 160 NaCl and 5 Na-phosphate (pH 7.45), prior to further treatments, as described below.

Cell lysis in percent was calculated by the following equation:

$$\%\ \text{Lysis} = (OD_s^{527} \cdot 100)/(OD_h \cdot DF_h), \quad (1)$$

Where OD is the optical density measured using a Gilford Response spectrophotometer at 527 or 540 nm, DF the dilution factor, s the sample, and h the hemolysate collected at $t = 0$. Samples with greater than 7% hemolysis were discarded.

Methemoglobin (metHb) was estimated from the ratio of the absorbances of treated samples at 500 and 540 nm (OD^{500}/OD^{540}) as described previously [26]. Cellular GSH (mmol/Lpc) was determined as:

$$GSH_{pc} = [OD_s^{412} \cdot DF_{GSH}/E_{mol}]/hct_s \quad (2)$$

where OD_s^{412} is the *OD* of the sample measured at 412 nm, DF_{GSH} the dilution factor for *GSH* determination (55X), E_{mol} = the molar extinction coefficient of *GSH* (14.0), Lpc = liter of packed cells and hct_s = hematocrit of the sample.

Cellular pH was measured with a Fisher Scientific Accumet pH meter 910 (Fisher Scientific, Pittsburgh, PA) and standard Accumet glass-body combination electrodes in frozen-thawed cell pellets, as described previously [53].

Li Treatments

External Li

To demonstrate the effects of external Li on K-Cl COT, washed LK SRBCs were pre-swollen to RCV equal to 1.2 (20% swelling) to activate K-Cl COT, in a solution containing (mM): 115 NMDG-NO_3 and 5 Na-phosphate for 20 min (227 mOsM, 37°C, pH 7.45). Cells were then resuspended at 5% *hct* and fluxed in a Cl solution containing (mM): 10 or 100 LiCl and 122 or 15 NMDG-Cl, 10 RbCl, and 5 Na-phosphate for

Rb influx determination (See below). In this protocol, NMDG replaced Na to avoid transport of Li through the Na/Na exchanger.

Na/Li Exchange

Li was loaded through the Na/Li exchanger at approximately 1 mmol/LOC × hr, without altering the internal K concentration, $[K]_i$ [44]. Loading with Li caused RBC swelling. Thus, the osmolality, at which loaded cells attained the control volume was determined by addition of sucrose and was 345 mOsM. Washed RBCs were incubated at 37°C in 345 mOsM solutions at 10% hct, containing (mM): for controls, 125 NaCl, 15 KCl, 5 Na-phosphate (pH 7.45), 10 glucose and sucrose; for Li-treated cells, 125 LiCl, 15 KCl, 5 Na-phosphate (pH 7.45), 10 glucose, and sucrose. All solutions contained 12 units penicillin/ml (0.1% total volume) and 12 μg streptomycin/ml (0.1% total volume). Afterwards, cells were swollen to 20% above isotonic volume by incubation at 37°C and 5% *hct* in hyposmotic solutions (240 mOsM for Cl and 227 mOsM for NO_3) containing (mM): 122 NMDG-Cl or 115 NMDG-NO_3, 5 Na-phosphate (pH 7.45), and 10 glucose. Internal cation concentrations of Na, Li, Rb and K were determined by atomic absorption or emission spectroscopy using a Perkin Elmer 5000 Spectrophotometer as previously described [24, 44].

Nystatin loading

Nystatin was used to load Li into LK SRBC as described previously [12, 20]. A nystatin stock solution containing 60 mg/ml nystatin in dimethylsulfoxide (DMSO) was freshly made. Washed cells were incubated for 30 min at 0°C in a 345 mOsM hyperosmotic loading solution (LS) containing (mM): 130 NaCl (for controls) or 130 LiCl (for Li-treated cells), 20 KCl, 5 Na-phosphate (pH 7.45), 10 glucose, sucrose and 60 μg/ml nystatin. Cells were then incubated for another 30 min at 0°C in the same LS without nystatin. To remove membrane-bound nystatin, cells were washed 7 times in warm (37°C) LS containing bovine serum albumin (BSA, 0.5 mg/ml) and 4 times in a BSA-free solution containing (mM): 122 NMDG-Cl (230 mOsM) or 115 NMDG-NO_3 (220 mOsM) and 5 Na-phosphate (pH 7.45) at 0°C. Compared to controls, nystatin-treated cells were shrunken and therefore were re-swollen in solutions of lower osmolality to maintain 1.2 RCV during preincubation and flux procedures.

K, Rb and Li Fluxes

Zero-trans K efflux was determined as described previously [12, 24]. Briefly, cells were preincubated at 10% *hct* for 20 min at 37°C, in a hyposmotic solution (227 mOsM) containing (mM): 115 NMDG-NO_3 and 5 Na-phosphate (pH 7.45). Warm flux solutions (37°C) containing (mM): 122 NMDG-Cl or 115 NMDG-NO_3 and 5 Na-phosphate (pH 7.45), were added to packed cells to obtain a final hct of 5%. Cells were incubated up to 60 min, samples were taken at 10 min intervals, placed immediately on ice and centrifuged up to 12,000 × *g* when the exact time was recorded. Supernatants were transferred to tubes containing 1/100th volume of a concentrated hemolysing solution (HS, 100X) (*see* below for HS composition). For Rb influx measurements, solutions contained (mM): 10 RbCl/NO_3, 140 NMDG-Cl or 132 NMDG-NO_3 and 5 Na-phosphate (pH 7.45). Samples of 0.15 ml pc were taken every 10 min and added to tubes containing 0.15 ml of cold $MgCl_2$ solution (295 mOsM) and 10 mM Tris-MOPS (pH 7.45 at 0°C). The tubes were immersed in iced water, and the cells washed twice with cold $MgCl_2$ solution by centrifugation at 6,000 × *g* followed by a final spin at 12,000 × *g* for 1 min. The packed cells were diluted 1:14 (v/v) with HS containing 0.01 mM NH_4OH, 4 mM CsCl, and 3% noncationic detergent Acationox (Baxter Health Care, McGraw Park, IL) [44] to determine Li by atomic absorption and Rb by emission. For all experiments, 10^{-4} M ouabain prepared from a 10^{-2} M stock solution in deionized water was added prior to fluxing. Flux data were expressed in mmol K, Rb or Li/[LCW × hr], based on determination of CW by the drying technique described previously [23].

Acute and Chronic Studies with Li and Modulators of the PKC-Dependent Pathway

Acute Studies

LK SRBCs were pre-incubated up to 1 hr in media of the following composition (mM): 125 NaCl or 125 LiCl, 15 KCl, 5 Na-phosphate (pH 7.45 at 37°C), 10 glucose, ± 100 nM TPA, or 50 μM PD98059, or 20 nM calyculin A, and sucrose to bring the osmolality to 345 mOsM. Flux solutions contained (mM): 122 NMDG-Cl (240 mOsM) or 115 NMDG-NO_3 (227 mOsM), 5 Na-phosphate (pH 7.45 at 37°C), and 10^{-4} M ouabain. TPA and PD98059 stock solutions were dissolved in DMSO and stored at −80 and −20°C, respectively. Calyculin A was dissolved in ethanol and stored at −80°C.

Chronic Studies

LK SRBCs were pre-incubated up to 20 hr in media of the following composition (mM): 125 NaCl or 125 LiCl, 15 KCl, 5 Na-phosphate, 15 PIPES/bicine (pH 7.45 at 37°C), 10 glucose ± 100 nM TPA, or ± 50 μM PD98059, or ± 20 nM calyculin A, and sucrose to bring osmolality to 345 mOsM. Flux solutions contained (mM): 122 NMDG-Cl (240 mOsM) or 115 NMDG-NO_3 (227 mOsM), 5 Na-phosphate (pH 7.45 at 37°C), and 10^{-4} M ouabain.

Morphological Studies

Changes in LK SRBC morphology were observed by microscopy. Digitized images were collected using a Hamamatsu model XC-77 CCD video camera module, CD2400 CCD camera control, frame grabber board and imaging software (Computer Eyes/RT Mono, v 5.12, Digital Vision, Dedham, MA), with a 100× magnification via Hoffman Modulation Contrast (HMC) optics. LK SRBCs were washed thrice in isosmotic solution, and preincubated in isosmotic or hyperosmotic solutions for 20 min at 37°C, pH 7.45 prior to resuspension in the test solution. Images of control and Li-treated cells were collected at 1 and 20 hr under isosmotic (295 mOsM) or hyperosmotic (345 mOsM) conditions. The isosmotic solution contained (mM): 125 NaCl or LiCl, 15 KCl, 5 Na-phosphate (pH 7.45), 15 PIPES/BICINE and 10 glucose (37°C). The osmolality of the hyperosmotic solution was adjusted with sucrose (pH 7.45, 37°C). Addition of the test solution was considered $t = 0$. Samples were taken as quickly as possible.

Protein Separation

Separation of phospholipids and their protein products were accomplished using procedures described previously, with modifications specific for the extraction of DAG [7, 10, 37, 48, 50]. Briefly, 0.5 ml (unity volume) of Li-treated or control packed cells (pc) were added dropwise to 5 ml of methanol (MeOH) at a 1:10 (v:v) ratio and vortexed for 10 sec. The same volume (5 ml) of chloroform ($CHCl_3$) was added to the suspension to give a final ratio of 1:10:10 (v:v:v) and the suspension was again vortexed for 3 min. A second 5 ml of $CHCl_3$ was added to give a volume ratio of 1:10:20 (v:v). Four volumes (two ml) of deionized water were added, the solution vortexed briefly, and then allowed to sit on ice, in the dark, for 5–10 min. The solution was centrifuged at 2,900 × *g* for 5 min and returned to ice for 5 min. The

MeOH-water extract contained the more polar substances, including the phospholipid inositol monophosphate, IP, while the $CHCl_3$ extracts contained the nonpolar substances including diacylglycerol, DAG. These organic layers, 7 ml of MeOH-water extract and 10 ml $CHCl_3$ extract, were carefully pipetted off and transferred to new containers. Two volumes (1 ml) of deionized water were added to the $CHCl_3$ extract to further separate out any remaining polar substances. The $CHCl_3$-water extraction mixture was vortexed briefly and kept on ice for 5 min to separate the layers. The aqueous layer formed from this second extraction was combined with the MeOH-water extract from the first extraction (total volume, 8 ml). To remove the contaminant Hb, the $CHCl_3$ extract was filtered through 0.5 ml of silica gel. Organic solvents were removed by evaporation in the dark for 16–20 hr. Samples from each extraction mixture were collected and run on a TLC slide preparation to verify the location of IP and DAG prior to large-scale chromatography. Data were expressed in terms of liters of original cells (LOC).

Thin Layer Chromatography (TLC)

Dried lipids were resuspended in 100 μl of either MeOH or $CHCl_3$ and spotted 2 cm apart on a TLC plate. Samples were run in parallel to a standard of 0.05 mg of either diolein or phosphatidylinositol (*See* Chemicals in Material and Methods for further details). Nonpolar lipids were developed in a solvent containing $CHCl_3$: MeOH: petroleum ether (PET): acetic acid (AA) in a ratio of 5:1.6:3:1 (by volume), as described previously [7, 37]. Polar solutions were developed in a modified solvent containing: $CHCl_3$: MeOH: PET: AA (11.6: 0.8:7: 0.5, by volume). Plates were dried by ventilation and exposed for 1 hr to iodine. The resultant *Rf* values (expressed as the mean ± SD) (n = 8) were 0.31 ± 0.01 for the PI standard, and 0.68 ± 0.06 for the diolein standard. The mean slope values (±SD) were 46.7 ± 0.9 average peak intensity (API)/0.1 mg of PI standard and 15.5 ± 0.28 API/0.01 mg of diolein standard.

Quantitation

Stained plates were analyzed by densitometry using Imagcalc, version 1 (C.H.A. van de Lest). Images were created using Photoshop version 4.0 (Adobe Systems), and the data were quantified using Excel version 6.0 (Microsoft). Peak intensity values of a grouping of ten vertical scans were averaged to calculate one data point. Calibration curves were created from the averaged peak intensities of three separate experiments, using standards of PI ranging from 0 to 0.25 mg and standards of diolein ranging from 0 to 0.08 mg. The rate of change in intensity (m), determined by linear regression, was a function of concentration for each standard used in the calculation of samples. The formula used to determine concentrations was: $Y = mX + b$, where Y is the average peak intensity, m, the slope of the calibration curve, X, the unknown concentration and b, the background intensity. This parameter was obtained for each plate by extrapolation of the standard intensities.

Calculation of the Kinetic Parameters K_m and V_{max}

The **Hanes** transformation of the Michaelis-Menten equation was applied to estimate K_m (i.e., the $[K]_i$ at which K efflux (v) was half maximally activated) and V_{max} (the maximum K flux):

$$[K]_i/v = K_m/V_{max} + [K]_i/V_{max}, \quad (3)$$

where V_{max} was calculated from 1/slope and $-K_m$ is the intercept with the x-axis. For estimation of the IC_{50} or the apparent K_i for Li, the **Dixon** plot of $1/v$ *vs.* $[Li]_i$ was used under the assumption of a simple type of inhibition:

$$v = V_{max}/(1 + [Li]_i/K_i^{app}). \quad (4)$$

Average K_m and V_{max} were calculated from a compilation of independent experiments. In each experiment, K efflux rate constants for each $[K]_i$ were calculated from 3–5 time points. Independent determinations of V_{max} and K_m were obtained for each experiment. Individual data points ($[K]_i$/K efflux) *vs.* $[K]_i$) were selected based on their adherence to a 95% predictability confidence curve obtained with all the individual values (whole population) according to Statistix version 4.0 (Analytic Software, St. Paul, MN). For calculation of individual parameters, points were omitted if their inclusion significantly altered (>3 SD) the calculated V_{max} and K_m values with respect to those of the whole population.

Statistical Analysis

The statistical significance of the results was determined by paired or unpaired two-population t-test at the $P < 0.05$ level, using the Microcal Origin 3.5 program (Microcal Software, Northampton, MA). Calibration curves were fitted by linear regression with the Origin 3.5 program (Microcal). Results were expressed as either the mean ± SE (X ± SE) or mean ± standard deviation (X ± SD).

Abbreviations/Symbols

Hct, hematocrit; TLC, thin layer chromatography; PL, phospholipase; GSH, glutathione; Hb, hemoglobin; metHb, methemoglobin; KCC, potassium-chloride cotransporter; LOC, liter of original cells; LCW, liter of cell water; RCV, relative cell volume; PKC, protein kinase C; Li, lithium; K, potassium; Rb, rubidium; Cl, chloride; NO_3, nitrate; PI, phosphatidylinositol; DAG, diacylglycerol; TPA, 12-o-tetradecanoylphorbol-13-acetate; MEK, mitogen activated protein kinase (ERK2) kinase; PP-1, protein phosphatase-1. Li_i, Li_o, K_i, K_o, PI_i, DAG_i, denote respective cation and substrate presence in the intracellular (i) or extracellular (o) compartments. Concentrations in these compartments are expressed as $[ion/substrate]_{i,o}$.

Results

Li Effects on Cell Volume

Previous studies showed that dog RBCs swelled when incubated in Li-salt solutions, an effect attributed to K-Cl COT inhibition due to an increase in the volume "set point" [38–40]. Therefore, the effect of Li was tested on RCV and morphology in LK SRBCs, prior to assessing the action of Li on K-Cl COT. As shown in Fig. 1, all cells incubated in LiCl for 1 or 20 hr in isosmotic or hyperosmotic solutions, had increased spindle and anthrocyte shape changes. The Table shows a 15% shrinkage for control LK SRBCs suspended in 345 mOsM compared to isosmotic controls at $t = 0$. In contrast, LK SRBCs in both isosmotic or hyperosmotic 130 mM LiCl media swelled about 14%, an effect also reported in dog

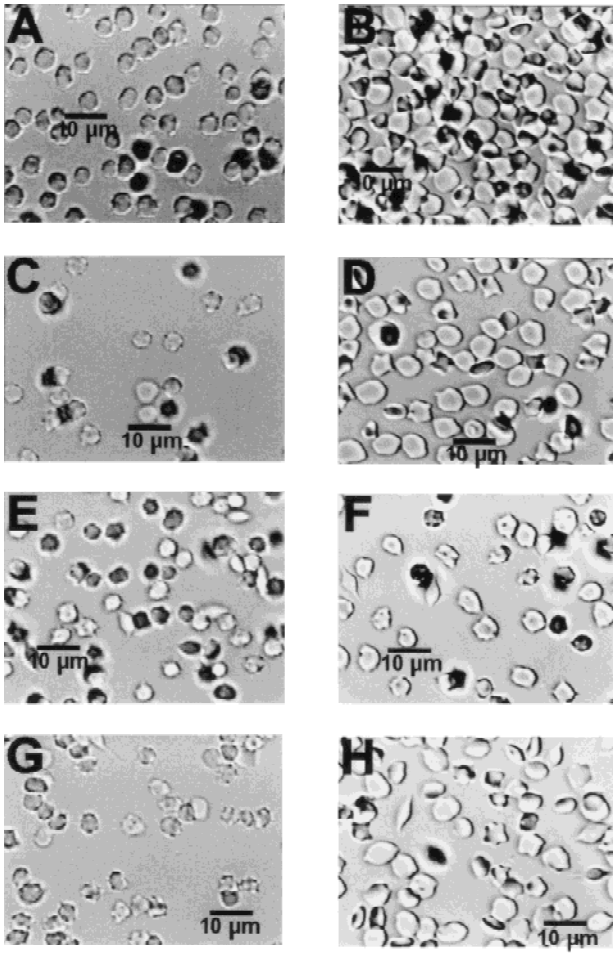

Fig. 1. Changes in morphology and cellular diameter of LK SRBCs in response to incubation in Li-containing solutions. Freeze frame images were collected and cellular diameters were determined as described in Materials and Methods. Panels *A* and *B:* 1 and 20 hr in isosmotic (295 mOsM) media. Panels *C* and *D:* 1 and 20 hr in Li-containing, isosmotic media. Panels *E* and *F:* 1 and 20 hr in hyperosmotic (345 mOsM) media. Panels *G* and *H:* 1 and 20 hr in Li-containing, hyperosmotic media. Average cell diameters ($n \geqslant 20$) were determined and used for statistical comparison between conditions. Similar results were obtained from 3 independent experiments.

RBCs [38]. The Table also reveals that the cellular diameters for controls were smaller in hyperosmotic media, though not significantly different from those in isosmotic solutions. Their diameters increased by 17.5% after 20 hr incubation, compared to the 1 hr values. Cells incubated in isosmotic LiCl solution swelled by an additional 10 and 20% above controls after 1 and 20 hr incubation, respectively, and lysed close to their critical hemolytic volume [32] of 2.3 KgCW/KgDCS (equivalent to 24% swelling). The diameters of the small fraction of cells that did not lyse during incubation in LiCl were not significantly different from 1 hr controls. In contrast, cells incubated for 1 hr in hyperosmotic LiCl solution had diameters significantly larger than the 1 hr controls, a result unchanged after 20 hr. Li had no effect on the pH_i of cells incubated at any of the osmolalities tested (345 to 240 mOsM, *data not shown*). Thus, the changes in cell volume were not due to changes in cellular pH. In subsequent experiments, LK SRBCs were first loaded with Li in hypertonic media (345 mOsM) (to avoid massive lysis and loss of a large proportion of the cell population), and then were incubated in hypotonic media (240 mOsM) (to stimulate K-Cl COT). This protocol differs from that used in studies with dog RBCs [38].

Action of Li on K and Rb Fluxes

Like other cations (Ca, Na, K and H), Li may alter K-Cl COT by binding to cationic sites (as it occurs in the Na/K APTase and Na/Na exchanger) or to allosteric effector sites (as in the Na/H exchanger) (11, 44, 47). To explore the mechanism of Li effects on RBC volume regulation, the sidedness of Li effects on K and Rb fluxes through K-Cl COT were studied.

External Li Effects on Rb Influx

The external effect of Li was tested by suspending preswollen cells in solutions with 10 and 100 mM LiCl prior to flux measurements. Rb influx (mmol Rb/LCW × hr) for control cells was 1.15 ± 0.20 ($n = 6$), 1.34 ± 0.08 for cells in 10 mM $[Li]_o$, and 1.10 ± 0.03 in 100 mM $[Li]_o$. The data indicate no significant effect of Li_o on swelling-activated Rb influx.

Internal Li Effects on K Efflux

Li was loaded into LK SRBCs by Na/Li exchange or nystatin. The Na/Li exchanger eliminates potential ionophore artifacts such as membrane damage (i.e., cholesterol loss [9]). In contrast, nystatin permits a quick increase of $[Li]_i$ to values above 20 mmol Li/LOC [44] without affecting K fluxes in LK SRBCs [18]. Since incubation of LK SRBCs in 295 mOsM Li solutions induced between 15–20% cell swelling within 10 min regardless of the $[Li]_i$ (*results not shown*), LK SRBCs were incubated in 345 mOsM media so that the final water content was 1.83 KgCW/KgDCS (RCV = 1.02).

Figure 2 shows K efflux in Li-loaded cells as a function of $[Li]_i$. In Fig. 2*A*, the ordinate represents total K efflux in either Cl (squares) or NO_3 (circles). In Fig. 2*B*, the Cl-dependent K efflux or K-Cl COT was calculated from data in panel *A*. In Cl but not NO_3 media, Li_i inhibited K efflux between 1 and 15 mM, plateauing thereafter (Fig. 2*A*), and independently of the loading procedure. Because of its therapeutic significance, we also tested the effect of 0–1.2 mM $[Li]_i$ [5]. At these low

Table 1. Effect of Li incubation on relative cell volume (RCV) at $t = 0$ and on cellular diameter (D) at $t = 1$ and 20 hr of incubation in LK SRBCs

Condition	(mOsM)	RCV < 0 hr	(n)	(P)	D (mm) $t = 1$	(n)	(P)	D (mm) $t = 20$	(n)	(P)
Control	295	1.03 ± 0.03	6	—	4.0 ± 0.22	20	—	4.7 ± 0.25	20	0.0001*
	345	0.85 ± 0.02	5	—	3.7 ± 0.22	20	—	4.6 ± 0.25	21	0.0001*
LiCl	295	1.14 ± 0.01	6	0.004#	4.5 ± 0.22	20	0.0001*	5.0 ± 0.25	20	NSD
(130 mM)	345	1.03 ± 0.04	4	0.005#	4.7 ± 0.35	22	0.0024*	5.0 ± 0.33	20	NSD

RCV and D, expressed as (mean ± SE).
Results shown correspond to a representative experiment. Similar results were obtained from 3 independent experiments.
(#) Values are significantly different with respect to the $t = 0$ control.
(*) Values are significantly different with respect to the 1 hr control.
NSD values are not significantly different with respect to the 20 hr control.

concentrations, Li_i, increased K efflux in Cl by 30% with no effect in NO_3 (Fig. 2*A*). As shown in Fig. 2*B*, Li_i (>3 mmol LCW) inhibited K-Cl COT reaching 85% at >14 mmol Li_i/LCW. The apparent K_i or IC_{50} was 7.9 mM $[Li]_i$ calculated from a Dixon plot (*see* insert). Figure 2*C* shows that the IC_{50} was 6.6 mM $[Li]_i$ for the calculated Li-sensitive component of the Cl-dependent K efflux (data from Fig. 2*B*). Thus Li_i inhibited swelling-stimulated K-Cl COT with an apparent K_i of ~7 mM $[Li]_i$, an effect independent of the Li loading regime.

Internal Li Effects on Swelling-Activated K flux

Lithium inhibits K-Cl COT in dog RBCs by increasing the volume "set point" [38–40], the cell volume at which K-Cl COT activity is zero [26, 39]. If Li_i alters the response of K-Cl COT to changes in cell volume, it should affect the relationship between K efflux in Cl and RCV. A previous study showed that the basal K efflux in NO_3 is not volume-dependent [26]. Thus, we used K effluxes in Cl as representative for K-Cl COT. Figure 3 shows K efflux in Cl as a function of RCV for control and Li-containing cells (21 mmol Li_i/LCW). Note that 0.8 RCV corresponds to shrunken and 1.3 to swollen cells. Li_i decreased the response of K efflux to cell swelling from 3.5 in controls to 2.2 (mmol K/LCW × hr)/0.1 RCV and right-shifted the curve towards higher RCV values. Thus, to transport K at the same rate as the controls, Li-loaded cells should be about 20% more swollen. In other words, at the same cell volume, control LK SRBCs transport K at twice the rate of Li-loaded cells.

Internal Li Effects on pH Dependence of K Fluxes

K-Cl COT in volume-clamped LK SRBCs is stimulated by slightly acid pH_o (6.8), with minima at pH_o 6 and pH_o 8 [28]. To explore the effect of Li on the volume response of K-Cl COT to changes in pH_o, LK SRBCs were loaded with 19 mmol Li_i/LCW, swollen to an initial RCV of 1.2 at pH_o 7.4, and incubated in solutions of varying pH_o. In Fig. 4, control cells exhibited a pH_o activation profile of K efflux in Cl similar to previous reports, with peak activation near pH_o 6.8 [28]. In Li-loaded cells, however, the response of K-Cl COT to changes in pH_o decreased by 41 and 32% at pH_o 7.2 and 7.4, respectively, compared to controls. This indicates a left shift in the pH response of K efflux in Cl towards lower pHs. Plotting the data of Fig. 4 in a relative scale for K efflux did not cancel the left shift, indicating that the shift was not due to a decrease in the maximum fluxes of Li-loaded cells. At pH_o 6.8 and 6.6, hemolysis was 4–7% and may have reduced the statistical significance. The insert to Fig. 4 shows the RCV of control and Li-containing cells as a function of pH_o. There was no significant difference in the pH_o—induced cell volume changes between control and Li-containing cells.

Internal Li Effects on V_{max} and K_m for the K_i Activation of K Efflux

To further characterize the Li-induced inhibition of swelling-activated K-Cl COT, the effects of Li_i on V_{max} and K_m of K efflux in Cl were studied in swollen (RCV = 1.2) LK SRBCs. Cells were preloaded with >14 mmol Li_i/LCW and 5–35 mmol K_i/LCW using nystatin. Swelling-activated K efflux was a hyperbolic function of $[K]_i$ for both control and Li-containing cells. Li_i inhibited swelling-stimulated K efflux in Cl, and decreased the apparent affinity for K_i. Figure 5 is a Hanes plot (Eq. 3 in Methods) of $[K]_i$/K efflux in control and Li-containing cells as a function of $[K]_i$. The V_{max} values for K efflux, calculated from the slopes of the lines, were 7.0 for controls and 4.0 mmol K_i/LCW × hr for Li-containing cells, i.e., a decrease of 43%. The K_m values were 61.5 for controls and 82.1 mmol K_i/LCW for Li-containing cells, equivalent to a 34% increase by Li. The average V_{max} values were (mean ± SE), 6.5 ± 0.4 for controls ($n = 3$), and 3.8 ± 0.3 (mmol/LCW × hr) for Li-treated cells ($n = 4$). The average K_m values were 57.4 ± 0.7 and 74.1 ± 3.3 mmol K_i/LCW for controls and Li-treated cells, respectively. Based on the two popula-

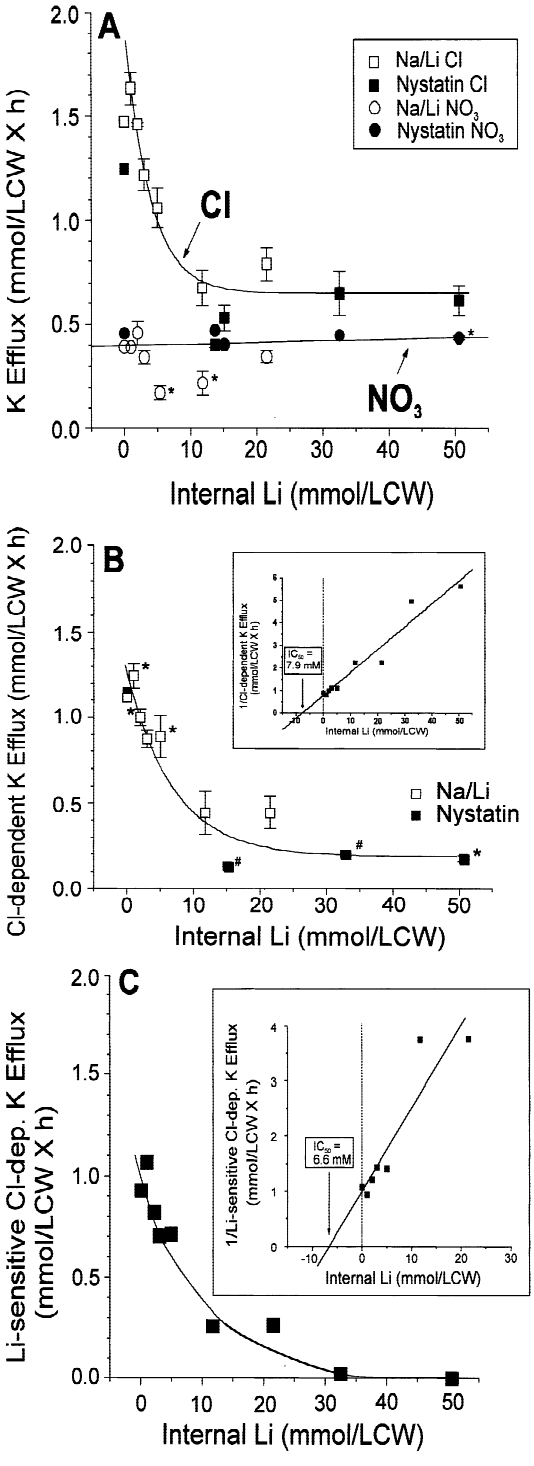

Fig. 2. Inhibition by Li of swelling-activated K-Cl COT in LK SRBCs. (*A*) Effect of Li on K efflux in hypotonic Cl and NO_3 media. Cells were loaded with 0–50 mmol internal Li (mmol/LCW (liter cell water) by Na/Li exchange (open symbols) or nystatin (closed symbols). For Cl (open and closed squares), data were fitted by exponential decay and for NO_3 (open and closed circles), data were fitted by linear regression, with an intercept at 0.40 mmol Li_i/LCW × hr. Error bars indicate ± standard error (SE) for $n = 3$–12 independent experiments. (*) represents the range for 2 independent experiments. (*B*) Effect of $[Li]_i$ on Cl-dependent K efflux in LK SRBCs. Li loading by the Na/Li exchanger (open squares, $n = 3$–4) or nystatin (solid squares, $n = 1$–3). Error bars are SE for $n = 3$–4 independent experiments. For $n < 3$, average values were plotted without error bars. Data were calculated from values in Fig. 2*A* and fitted by exponential decay. All cells were at 1.2 RCV. *Insert:* Dixon plot of 1/swelling-activated Cl-dependent K efflux versus $[Li]_i$ (closed squares). Data points were calculated from Fig. 2*B*. (*C*) Li-sensitive component of the swelling activated Cl-dependent K efflux versus $[Li]_i$ (closed squares). Data were derived from values in Fig. 2*A* and *B* and fitted by exponential decay. *Insert:* Dixon plot of 1/Li-sensitive, Cl-dependent K efflux versus $[Li]_i$ (closed squares). Data points were calculated from Fig. 2*C*.

tion unpaired *t*-test, both V_{max} and K_m values for Li-treated cells were significantly different from control values ($P = 0.003$ and 0.008, respectively). The combined results indicate a "mixed" noncompetitive inhibition by Li_i.

A "mixed" noncompetitive inhibition of K-Cl COT by Li_i may be explained by competition for K_i binding sites on the transporter. To test for this possibility, the fractional Li loss as a function of the $[Li]_i$ in either Cl or NO_3 was measured. A significantly greater loss of Li occurred in NO_3 as opposed to Cl. The rate constants of Li efflux in cells loaded with 13.6 ± 0.03 mmol/LOC Li_i were (hr^{-1}): 0.019 ± 0.001 in Cl, and 0.038 ± 0.003 in NO_3 ($P = 0.0002$, $n = 6$). Thus, cells lost Li at a rate

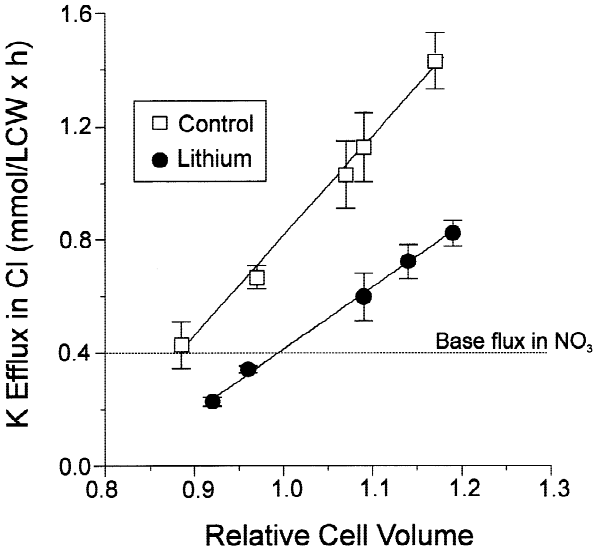

Fig. 3. K efflux in Cl for control and Li-containing cells as a function of relative cell volume (RCV). Experimental LK SRBCs cells contained 21.2 ± 1.3 mmol Li_i/LCW loaded by either the Na/Li exchanger or nystatin. Values were grouped by RCV for controls (open squares) and for Li-containing cells (solid circles); means ± SE for 3–6 independent experiments were calculated. Data were fitted by linear regression. The relationship between K efflux in Cl and RCV exhibited a slope of 3.5 ± 0.1 standard deviation (SD) ($R = 0.998$) for controls and 2.2 ± 0.1 (mmol/LCW × hr)/0.1 RCV ($R = 0.999$) for Li-containing cells. The stippled, horizontal line defines the base flux in NO_3 as measured at 1.2 RCV in Fig. 2*A*.

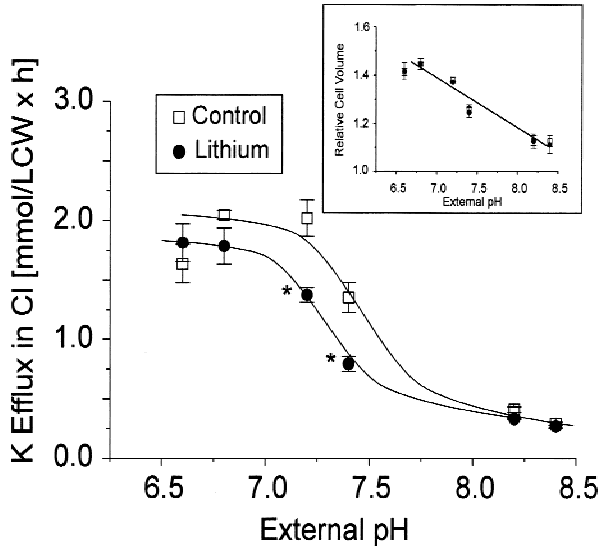

Fig. 4. Effect of Li_i on the response of K-Cl COT to changes in pH_o in LK SRBCs. Li was loaded by the Na/Li exchanger or nystatin to 18.6 ± 0.9 mmol Li_i/LCW. K efflux values for control (open squares) and Li-containing cells (closed circles) are expressed as the means ± SE. K efflux for Li-containing cells at pH_os 7.2 and 7.4 were significantly lower [($P = 0.007$, $n = 4$) and ($P = 0.016$, $n = 3$)], respectively, than their controls as determined by the two population paired *t*-test (*). *Insert:* RCV ± SE of control (open squares) and Li-containing (closed circles) LK SRBCs *vs.* external pH (initial RCV was 1.2).

of about ⅓th of that of K loss in Cl. In NO_3, the rate of Li loss was of similar magnitude to that of K.

Increased metHb formation and decreased GSH concentration are indicators of increased cellular oxidation, known to be associated with stimulation of K-Cl COT [2, 29]. Long-term incubation of LK SRBCs in the absence of Li (control cells) revealed a characteristic red to brown color change (metHb formation) likely associated with cellular oxidation. In contrast, Li-loaded cells remained bright red. To test whether Li_i inhibition of swelling-activated K-Cl COT was due to modification of the redox-state of the cell, GSH was measured. However, neither cellular GSH nor metHb formation were significantly altered when compared to controls (*data not shown*). Thus, these results could not explain the lack of Hb oxidation (observed in the long-term incubations) in Li-loaded cells.

Internal Li Effects on Phospholipid Turnover

In skate RBCs, cell swelling induces DAG formation, indicating that the PI turnover pathway may be involved in RVD [31]. PI participates in two ways in the cycle: one, as an intermediate of the cycle itself, and the other through a second pool in the cytoskeleton [10]. DAG and inositol-1, 4, 5-triphosphate (IP_3) are the two end products of the turnover pathway. IP_3 is hydrolyzed into an intermediate of the cycle. In contrast, DAG breaks down into phosphatidic acid (PA), which is not an intermediate of the PI pathway. There are 4 potential sources for DAG formation: (i) 1-phosphatidyl-3, 5-inositol bisphosphate (PIP2) hydrolysis by phospholipase C (PLC); (ii) direct PI hydrolysis by PLC; (iii) direct hydrolysis of phosphatidylcholine (PC) by PLC; and (iv) phospholipase D (PLD)-associated formation of PA, followed by conversion to DAG by phosphatidate phosphohydrolase [41]. Since the presence of DAG and IP_3 is not sufficient evidence to postulate a complete PI turnover pathway, a known effector of the pathway must induce predictable changes to support this hypothesis. Li alters the PI turnover pathway in human erythrocytes by inhibiting myo-inositol monophosphatase, which by converting inositol monophosphate (IP) into myo-inositol [42], decreases cellular PI and increases DAG. In contrast, Li does not alter DAG production through the PLD pathway. Thus, Li-dependent changes in PI and DAG concentrations would uncover the presence of a complete PI turnover cycle in LK SRBCs.

DAG and $[PI]_i$ were determined in swollen (1.2 RCV) LK SRBCs. Figure 6*A* presents changes in $[PI]_i$ in control (open squares) and Li-containing cells (closed circles) loaded by Na/Li exchange. The incubation time in h equals $[Li]_i$ (mmol/LOC) as indicated on the ab-

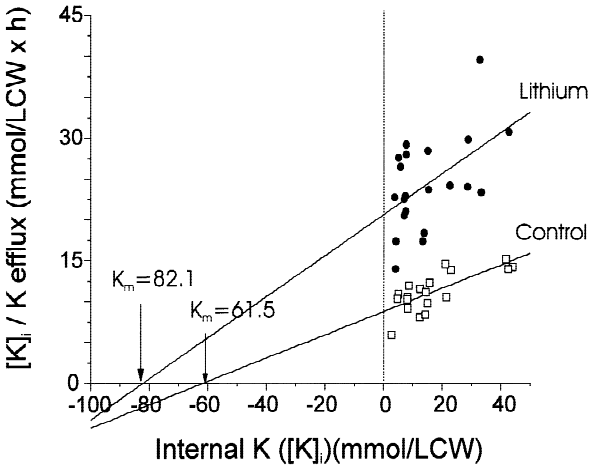

Fig. 5. Hanes Plot of the effect of Li on V_{max} and K_m. Plotted is the ratio of $[K]_i$/K efflux in Cl for control and Li-containing LK SRBCs as a function of $[K]_i$. For control cells (open squares) $n = 19$, $V_{max} = 7.0$ mmol K_i/LCW × hr, and $K_m = 61.5$ mmol K_i/LCW. For Li-containing cells (solid circles) n = 21, $V_{max} = 4.0$ mmol K_i/LCW × hr and $K_m = 82.1$ mmol K_i/LCW. Statistical significance was determined by two population-unpaired *t*-tests. Individual experiments included 3–5 time points. Values for kinetic parameters were based on their adherence to a 95% predictability confidence curve. For calculations on independent experiments, values were omitted if their inclusion significantly (>3 STD) altered the calculated V_{max} and K_m values determined for the total sample.

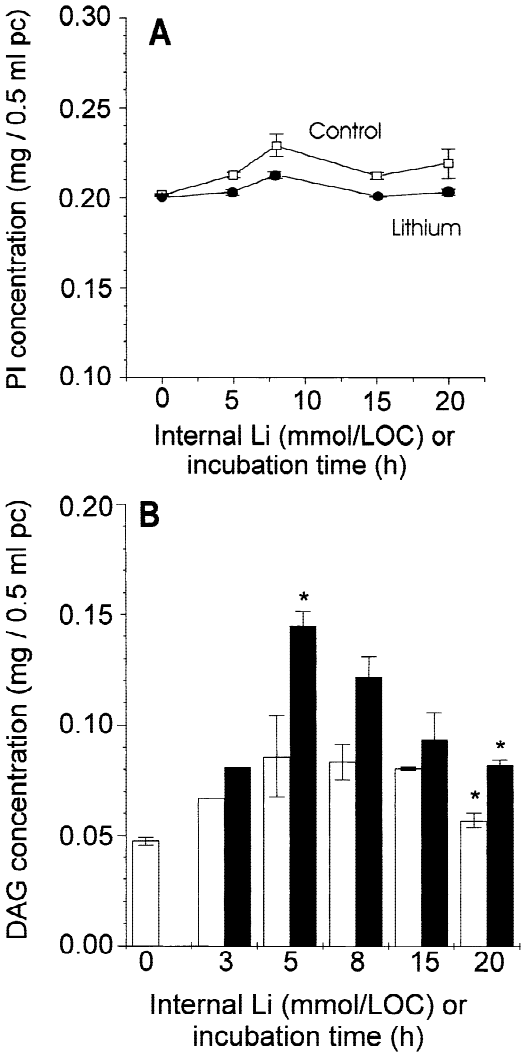

Fig. 6. Phosphatidylinositol (PI) and diacylglycerol (DAG) concentration in LK SRBCs as a function of $[Li]_i$ or incubation time in hyposmotic solution. (*A*) Effect of $[Li]_i$ and time on PI concentration. Data are the means ± range of 2 independent experiments for control cells (open squares) and Li-containing cells (solid circles) at RCVs of 1.2. (*B*) Effect of $[Li]_i$ and time on DAG concentration. Data are the means ± SE for 3 independent experiments or the mean for $n = 2$. Open columns for controls and filled columns for Li-containing cells. Asterisks (*) denote values significantly different ($P < 0.05$) for both initial controls as well as from the average of comparable control values.

scissa of Fig. 6*A*. The upper trace for $[PI]_i$ in controls as well as the lower for Li-containing cells as a function of incubation time (hr) was about 0.2 mg/0.5 ml pc. The lack of significant changes in $[PI]_i$ with increased $[Li]_i$ is possibly due to the fact that PI is better buffered (it has more than one source in RBCs, where the cytoskeleton harbors several PI intermediates) and is present at concentrations between 1.3- to 4-fold higher than DAG. These factors together with the low sensitivity of the method, may not allow for detectable changes in $[PI]_i$, even though Li decreased PI by 0.8, 4.5, 8.0, 5.6 and 7.8%, with respect to controls, at 0, 5, 8, 15 and 20 hr, respectively. Furthermore, taking the change at 0 time as a reference (i.e., $[PI]_i$ in Li-loaded cells-$[PI]_i$ in control cells), the decrease in PI induced by Li as a function of time was: 0, 435, 847, 665 and 929% at 0, 5, 8, 15 and 20 hr, respectively.

Figure 6*B* shows the changes in $[DAG]_i$ in mg/0.5 ml pc as a function of incubation time (hr) for controls (open columns) and of $[Li]_i$ for Li-containing cells (filled columns). In controls, $[DAG]_i$ increased by 84% after 5 hr, from 0.045 ± 0.002 to 0.083 ± 0.018, with respect to initial values ($P = 0.0001$). Between 5 and 15 hr, the control $[DAG]_i$ remained unchanged. At 20 hr, $[DAG]_i$ decreased slightly, but remained still different from initial values ($P = 0.032$). In Li-treated cells, $[DAG]_i$ increased beyond the controls: at 5 mmol $[Li]_i$, by 81% (to 0.145 ± 0.006 mg/0.5 ml pc) as compared to the 5 hr control values (0.083 ± 0.018 mg/0.5 ml pc, $P = 0.0001$), and at 20 mmol $[Li]_i$, $[DAG]_i$ was still 0.080 ± 0.002 mg/0.5 ml pc, significantly greater than the 20 hr control (0.058 ± 0.003 mg/0.5 ml pc, $P = 0.001$).

In summary, the presence of the two components of the PI turnover cycle, PI and DAG, and the sensitivity of DAG formation to changes in $[Li]_i$, suggest that LK SRBCs possess a complete PI cycle. The DAG formation responded in a bimodal fashion to increasing $[Li]_i$ and was significantly greater than controls at all $[Li]_i$ and

time points tested. However, $[PI]_i$ was not significantly altered by Li_i. No correlation was found between K efflux in Cl and DAG formation as a function of $[Li]_i$, perhaps because DAG, as a second messenger, has an independent downregulatory mechanism [41].

Internal Li Effects on K-Cl COT and PKC-Dependent Pathway

Phorbol esters such as TPA (400 nM) are commonly used for short-term (acute, 1–10 min) exposure to stimulate PKC [49]. TPA is used at higher concentrations (>400 nM) and long-term (chronic, 24 hr) exposure to induce irreversible downregulation of PKC [49]. The mechanism of PKC-stimulation by TPA is through competition with DAG for binding to the enzyme, causing increased PKC translocation and phosphorylation. TPA stimulates PP-1 activity in a time- and dose-dependent fashion through a PKC-dependent pathway, facilitating MAPK phosphorylation of PP-1 [49]. Okadaic acid and calyculin A inhibit PP-1 phosphatase and swelling-activated K-Cl COT [19, 22]. Based on these studies and the effect of Li on the PI cycle shown above, we tested whether in LK SRBCs, Li_i modulates swelling-activated K-Cl COT through a PKC-dependent kinase/phosphatase cascade, which includes MAPK and PP-1.

Acute or chronic time-dependent effects of TPA, PD98059, a MEK inhibitor, and calyculin A were determined on cellular morphology and swelling-activated K-Cl COT in control and in cells loaded with Li by Na/Li exchange. As shown for Li (Fig. 2), incubation in the presence of TPA (100 nM) or PD98059 (50 μM) modified cellular morphology (*data not shown*). After 1 hr, K-Cl COT increased in Li- (at 1 mmol/LOC) and TPA-treated cells by 25 and 38%, respectively, ($P = 0.002$, $n = 4$, *results not shown*). In another set of experiments, Li caused 9 and 27% increases in K-Cl COT at 30 and 60 min, respectively, and TPA 7, 24 and 40% increases at 10, 30 and 60 min, respectively, above their controls. In contrast, 30-min incubation of LK SRBCs with calyculin A inhibited K-Cl COT by 71%.

To simultaneously test the chronic effect of Li and TPA, LK SRBCs were pretreated for up to 20 hr in the presence and absence of Li (125 mM) or 100 nM TPA, followed by 20 min incubation in hyposmotic media prior to flux measurements. Li modified K-Cl COT as previously shown in Fig. 2*A–C*. Likewise, TPA affected the swelling-activated K-Cl COT in a bimodal fashion, as it was observed for Li-loaded cells in Fig. 2*B*. Stimulation of K-Cl COT by TPA occurred between 0 to 60 min, was maximal (approximately 35% above controls) at 1 hr, and declined to controls after 3 hr. On average, 1 hr incubation with Li (1 mmol/LOC) ($n = 4$) or TPA ($n = 3$) stimulated swelling-activated K-Cl COT by 30%. At 1 hr, K-Cl COT in Li- and TPA-treated cells was significantly greater than controls ($n = 4$) ($P < 0.0002$) but not different from each other. Beyond 3 mmol Li/LCW or 3-hr incubation with TPA, K-Cl COT was concentration- or time-dependently inhibited with an IC_{50} of ~8 mM Li/LCW (as in Fig. 2*B*) equivalent to 8 hr incubation in 100 nM TPA (TPA *data not shown*). K-Cl COT was 50% inhibited in cells containing 20 mmol Li/LOC or incubated for 20 hr in TPA.

To test the effect of PD98059 (a MEK inhibitor) and calyculin A (a PP-1 inhibitor) on K-Cl COT, LK SRBCs were preincubated in hypertonic medium (345 mOsM), in the presence and absence of 50 μM PD98059 or 20 nM calyculin A for 3 hr. K loss was determined as a function of time in hypotonic medium (240 mOsM for Cl and 227 mOsM for NO_3). Preliminary studies showed no effect of these inhibitors on K loss in NO_3. The K efflux rate constants (hr^{-1}) were (mean ± SD, n_1, n_2, number of points for rate constant determination and number of independent experiments, respectively): 0.092 ± 0.023 (4, 1) in Cl; 0.024 ± 0.002 (4, 1) in NO_3; 0.059 ± 0.001 (17, 3) in Cl + PD89059; and 0.029 ± 0.001 (13, 3) in Cl and Calyculin A. Thus, PD89059 and calyculin A inhibited swelling-activated K-Cl COT by 48 and 92%, respectively. Similar results were obtained in a separate set of experiments, in which LK SRBCs were incubated for 2 hr in Cl and NO_3 ± PD98059 and ± calyculin A. PD98059 and calyculin A inhibited K loss in Cl by 59%, $P = 0.015$, $n = 3$, and by 73%, $P = 0.002$, $n = 3$, respectively. No effect was observed in NO_3. Furthermore, they inhibited the swelling-activated K-Cl COT by 50% ($P = 0.01$) (PD89059) and 100% (calyculin A) (*results not shown*). Incubation for up to 300 min in the presence and absence of 50 μM PD98059 inhibited K-Cl COT by 34 to 80% between 60 and 300 min, respectively ($n = 2$, *results not shown*).

The above results suggest that Li and TPA modulate K-Cl COT through a similar pathway. Based on the action of TPA on PKC, these results point to an association between a PKC-dependent pathway and K-Cl COT. The PKC-dependent pathway includes MAPK kinase (inhibited by PD98059), and PP-1 (inhibited by calyculin A). Thus, K-Cl COT was modulated or inhibited by all the tested agents (bimodal effect of Li and TPA, and inhibition by PD98059 and calyculin A).

In conclusion, our study confirms the findings by Parker and others [38–40] that Li-inhibits swelling-activated K-Cl COT and reduces its volume sensitivity. This study reports for the first time that Li alters the response of swelling-activated K-Cl COT to changes in pH. Furthermore, TPA and PD98059 inhibited K efflux in Cl, and therefore implicate a PKC-dependent pathway in swelling-activated K-Cl COT, identifying putative upstream components of the regulatory pathway. This study also validates a new TLC protocol for the quanti-

tative determination of cellular PI and DAG and thus is the first report of the presence of a complete PI turnover pathway in LK SRBCs.

Discussion

Our study examined the relationship between K-Cl COT activity, cellular morphology, cell volume, and DAG production to determine the mechanism of Li action on the transporter and its regulatory pathways.

The Li-induced rapid cellular swelling and spindle or anthrocyte formation of LK SRBCs (Fig. 1) were not the result of changes in pH_i. Internal but not external Li inhibited the swelling-activated K-Cl COT with an IC_{50} of ~8 mM $[Li]_i$ and by a "mixed" noncompetitive mechanism (Figs. 2*B, C* and 5). In Cl, Li_i decreased K efflux in the entire range of osmolalities tested (*see* right shift in Fig. 3) and decreased the response of K efflux to changes in pH_o (*see* left shift in Fig. 4). The decrease of K efflux by Li occurred without affecting pH_o-induced cell volume changes (Insert Fig. 4) or the metabolism-dependent oxidative state of the cells. Furthermore, Li modulated DAG production in a bimodal fashion through the PI turnover cycle (Fig. 6*B*), without significantly affecting the cellular PI concentration (Fig. 6*A*).

Incubation in Li solutions resulted in fast (within <10 min) changes in cell volume and morphology (Fig. 1), not correlated with the $[Li]_i$ and similar to those observed in HeLa cells [30]. Because HeLa cells are immortal leukemic cells with myeloid characteristics, they may resemble other hematopoietic progenitors (i.e., of red blood cells). The mechanism by which Li alters cell morphology is not clear. Hematopoietic cells may have extracellular sites for Li binding mediating cell swelling and cytoskeletal deformation. Despite swelling (Table 1), the cells exposed to Li displayed spindle and anthrocytic forms ruling out a correlation between cell volume and the Li-induced morphological changes. Furthermore, although Parker [38] speculated that cell swelling may be the result of inhibition of K-Cl COT by Li, we found no correlation between Li-effected changes in cell volume and K-Cl COT activity (Table 1 and Fig. 3).

Li_i inhibited K efflux in Cl by 39%, inducing a right shift towards higher RCVs (Fig. 3). These results suggest that Li-treatment interferes with the mechanism that turns on the K-Cl COT volume regulatory pathway. The response of K-Cl COT to cell volume changes may involve the effect of ions on the transporter itself, on the regulatory cascade or on both. For example, like Li, thiocyanate (SCN) shifts the response of K-Cl COT to cell volume changes towards higher osmolalities [26]. Whether the observed effects are ionic in nature or a function of molecular crowding [39], remains to be determined. Ionic effects on K-Cl COT are well known in trout RBCs [17]. However, in SRBCs, these effects appear to play a more significant role in anion selectivity than in K-Cl COT regulation [26].

Li_i modified the characteristic bell shaped acid-activation curve for K-Cl COT [28, 53]. Control cells showed a maximum K efflux between pHs 6.8 and 7, which shifted to pHs 6.6 and 6.8 in Li-containing cells (Fig. 4). The nature of the putative site where Li could act is unknown. It is interesting to note, however, that quinine and quinidine, both positively charged molecules, inhibit K-Cl COT in LK SRBCS [1], and that protons inhibit K-Cl COT through an unidentified proton "sensor" [28]. It is conceivable that Li, the smallest monovalent cation, could act through this putative pH "sensor". In human RBC ghosts, positively charged polyamines exert similar effects, presumably by binding to negatively charged phospholipids on the cytoplasmic side of the membrane [45]. The effects of cations, including Li, on K-Cl COT may point to the involvement of negatively charged cytosolic components participating in or influencing the PI turnover cycle and the associated PKC-dependent pathway/s (*see* below). Thus, the action of Li on K-Cl COT may be indirect.

The effects of Li_i on the kinetic parameters (K_m and V_{max}) of swelling-activated K-Cl COT in LK SRBCs (Fig. 6) were of a complex nature. Thus, the "mixed" noncompetitive inhibition of K-Cl COT by Li_i may reflect its action on cytosolic components regulating the transporter. However, this form of inhibition does not rule out Li action at an allosteric site on the transporter that alters its conformation and ability to bind K. This effect may explain the increase in K_m and the significant decrease in V_{max} for K efflux in Cl. The fact that the inhibition of K-Cl COT was never "competitive" only proves that Li was not acting directly at the K binding site of the transporter. Moreover, Li was not carried on a Cl-dependent pathway. Instead, Li appears to move through a predominantly "NO_3-dependent" pathway. The Li leak pathway in LK SRBCs is unknown but may be related to a Cl-independent, Ca-dependent pathway for K transport (K_{Ca}) recently observed in mature LK SRBCs [35]. Alternatively, it may represent the Li leak pathway observed in resealed human RBC ghosts [46].

In humans, Li is known to inhibit myo-inositol 1-phosphatase, an enzyme of the PI cycle, without affecting other DAG forming pathways (i.e., phospholipase D (PLD) activity). The bimodal production of DAG with increasing $[Li]_i$ (Fig. 6*B*) suggests the presence of a complete PI cycle. The Li-induced bimodal response of K-Cl COT further indicates a cytosolic site for Li action within the regulatory pathway. In this study, the $[PI]_i$ was not significantly affected by Li_i (Fig. 6*A*), as seen in rat hepatocytes [6]. The observed results in SRBCs may be due to the fact that there are two ways in which PI may contribute to the cycle: one, as an intermediate of the cycle itself, and the other from a second

pool in the cytoskeleton. DAG, however, is a PI turnover product and can be formed either from the direct hydrolysis of PI intermediates and of phosphatidylcholine (PC) or by PA conversion by phosphatidate phosphohydrolase [41]. Of these possibilities, Li is known to affect only those pathways that involve PI turnover intermediates. As DAG is a second messenger for the PKC signal transduction pathway, its potential role in the regulation of swelling-activated K-Cl COT justified consideration, in particular, since earlier work did not clearly address this issue. The modulation by TPA and inhibition by PD98059 (*see* Results) suggests participation of a PKC-dependent pathway in K-Cl COT regulation.

Studies on skate RBCs [31], showing that incubation in 10 mM $[Li]_i$ for 30 min did not significantly affect PI turnover intermediates or product formation, appear to contradict our findings. The Li load occurring in that short period of time was less than the level of ~1 mM $[Li]_i$ used therapeutically in manic bipolar depression. Therefore, no Li effect would be expected based on the data shown in Fig. 2. In addition, differences between skate and sheep erythrocytes, amongst them nucleation, may account for some interspecies variability. However, in support of the data presented in Fig. 6*B*, it was shown that swelling of skate RBCs increased DAG, presumably through changes in PLC activity and phospholipid turnover [31]. Later, it was reported that the swelling-induced increase in $[DAG]_i$ involves PC hydrolysis and the PLD pathway [34]. In support of the data presented in Fig. 6*A*, inositol 1-monophosphate in skate RBCs increases during swelling, suggesting a potential decrease in $[PI]_i$ although it was not measured [31]. Studies involving human skin fibroblasts show that high-density lipoprotein 3 stimulates multiple signaling pathways simultaneously, including the PC-specific PLD pathway and the PC-specific PLC pathway, both of which lead to increased DAG formation [52]. The bimodal response of DAG formation induced by swelling and Li treatment (Fig. 6*B*) may be due to an initial activation of the PC-PLD pathway followed by a sustained increase in the activity of the PC-PLC pathway. At high $[Li]_i$, DAG production decreased again (Fig. 6*B*), perhaps in response to an increase in the activity of the DAG kinase or a PKC-mediated negative feedback on PLC as described previously [41].

In conclusion, Li may act both directly (at the transporter level) and indirectly (through a regulatory pathway). The direct effect of Li on the transporter may be at a site different from that for K binding, but which alters the conformation of the transporter and interferes with the binding of K (as reflected in an increase in K_m and a decrease in V_{max}). Alternatively, Li may decrease the number of active transporters, and through this mechanism, decrease the V_{max}. The Li-induced inhibition of swelling-activated K-Cl COT may involve a PKC-dependent regulation pathway. Li may effect this PKC-pathway indirectly, with and IC_{50} of 7 mM, through modification of DAG production and thus elicit a change in the transporter's response to pH and cell volume.

This work was in part supported by National Institutes of Health grant DK 37,160, National American Heart Association grant 0050451N, and in part by the Biomedical Sciences Ph.D. Program in fulfillment of C.M. Ferrell's Ph.D. thesis. We thank Dr. Olga Ortiz-Carranza for her guidance in experimental designs, Dr. Jay Dean for his help in acquiring the images captured by freeze frame photography, Dr. Julian Gomez-Cambronero for input on MAPK involvement, and Ms. Kathleen Rainey for her help with experimental details.

References

1. Adragna, N.C., Lauf, P.K. 1994. Quinine and quinidine inhibit and reveal heterogeneity of K-Cl cotransport in low K sheep erythrocytes. *J. Membrane Biol.* **142:**195–207
2. Adragna, N.C., Lauf, P.K. 1997. Oxidative activation of KCl cotransport by diamide in erythrocytes from humans with red cell disorders, and from several other mammalian species. *J. Membrane Biol.* **155:**207–217
3. Adragna, N.C., Lauf, P.K. 1998. Role of nitrite, a nitric oxide derivative, in K-Cl cotransport activation of low-potassium sheep red blood cells. *J. Membrane Biol.* **166:**157–167
4. Adragna, N.C., White, R.E., Orlov, S.N., Lauf, P.K. 2000. K-Cl cotransport in vascular smooth muscle and erythrocytes: possible implication in vasodilation. *Am. J. Physiol.* **278:**C381–C390
5. Agam, G., Livne, A. 1989. Inositol-1-phosphatase of human erythrocytes is inhibited by therapeutic lithium concentration. *Psychol. Res.* **27:**217–224
6. Allan, C.J., Exton, J.H. 1993. Quantification of inositol phospholipid breakdown in isolated rat hepatocytes. *Biochem. J.* **290:**865–872
7. Ansell, G.B., Dawson, R.M.C., Hawthorne, J.N. 1973. *In:* Form and Function of Phospholipids. pp: 43–65. Elsevier Scientific Publishing, Amsterdam, Netherlands
8. Bize, I., Dunham, P.B. 1994. Staurosporine, a protein kinase inhibitor, activates KCl cotransport in LK sheep erythrocytes. *Am. J. Physiol.* **266:**C759–C770
9. Bolard, J. 1986. How do the polyene macrolide antibiotics affect the cellular membrane properties. *Biochem. Biophys. Acta* **864:**257–304
10. Clark J.M. 1964. Experimental Biochemistry. Appendix II. W.H. Freeman, San Francisco and London
11. Davis, B.A., Hogan, E.M., Boron, W.F. 1992. Activation of Na-H exchange by intracellular lithium in barnacle muscle cells. *Am. J. Physiol.* **263:**C246–C256
12. Delpire, E., Lauf, P.K. 1991. Kinetics of Cl-dependent K fluxes in hyposmotically swollen low K sheep erythrocytes. *J. Gen. Physiol.* **97:**173–193
13. Dunham, P.B., Ellory, J.C. 1981. Passive potassium transport in low potassium sheep red cells; dependence on cell volume and chloride. *J. Physiol.* **318:**511–530
14. Elabbadi, N., Ancelin, M.L., Vial, H.J. 1994. Characterization of phosphatidylinositol synthase and evidence of a polyphosphoinositide cycle in Plasmodium-infected erythrocytes. *Mol. Biochem. Parasitol.* **63:**179–192
15. Flatman, P.W., Adragna, N.C., Lauf, P.K. 1996. Role of protein kinase in regulating sheep erythrocyte KCl cotransport. *Am. J. Physiol.* **271:**C255–C263

16. Gillen, C.M., Brill, S., Payne, J.A., Forbush III, B. 1996. Molecular cloning and functional expression of the KCl cotransporter from rabbit, rat and human. *J. Biol. Chem.* **271:**16237–16244
17. Guisouran H., Motais, R. 1999. Swelling activation of transport pathways in erythrocytes: effects of Cl^-, ionic strength, and volume changes. *Am. J. Physiol.* **276:**C210–C220
18. Grey, J.E., Lauf, P.K. 1980. Membrane cholesterol depletion and K transport in high and low potassium sheep red cells. *Membr. Biochem.* **3:**21–35
19. Jennings, M.L., Al-Rohil, N. 1990. Kinetics of activation and inactivation of swelling-stimulated KCl transport. The volume-sensitive parameter is the rate constant for inactivation. *J. Gen. Physiol.* **95:**1021–1040
20. Joiner, C.H., Lauf, P.K. 1978. Modulation of ouabain binding and potassium pump fluxes by cellular sodium and potassium in human and sheep erythrocytes. *J. Physiol.* **283:**177–196
21. Kaji, D.M. 1986. Volume sensitive K transport in human erythrocytes. *J. Gen. Physiol.* **88:**719–738
22. Kaji, D.M., Tsukitani, Y. 1991. Role of protein phosphatase in activation of KCl cotransport in human erythrocytes. *Am. J. Physiol.* **260:**C176–C180
23. Lauf, P.K. 1982. Evidence for a chloride-dependent potassium and water transport induced by hypo-osmotic stress in erythrocytes of the marine teleost Opsanus tau. *J. Comp. Physiol.* **146:**9–16
24. Lauf, P.K. 1983. Thiol-dependent passive K/Cl transport in sheep red cells. I. Dependence on chloride and external K [Rb] ions. *J. Membrane Biol.* **73:**237–246
25. Lauf, P.K. Thiol-dependent KCl transport in sheep red cells. IV. 1984. Furosemide inhibition as a function of external Rb, Na and Cl. *J. Membrane Biol.* **77:**57–82
26. Lauf, P.K. 1991. Foreign anions modulate volume set point of sheep erythrocyte KCl cotransport. *Am. J. Physiol.* **260:**C503–C512
27. Lauf, P.K., Adragna, N.C. 1996. A thermodynamic study of electroneutral K-Cl cotransport in pH and volume-clamped low K sheep erythrocytes with normal and low internal magnesium. *J. Gen. Physiol.* **108:**341–350
28. Lauf, P.K., Adragna, N.C. 1998. Functional evidence for a pH sensor of erythrocyte KCl cotransport through inhibition by internal protons and diethylpyrocarbonate. *Cell Physiol. Biochem.* **8:**46–60
29. Lauf, P.K., Bauer, J., Adragna, N.C., Fujise, H., Zade-Oppen, A.M.M., Ryu, K.H., Delpire, E. 1992. Erythrocyte K-Cl cotransport: properties and regulation. *Am. J. Physiol.* **263:**C917–C932
30. Matthopoulos, D.P., Tzaphlidou, M., Leontiou, I. 1995. Morphological alterations caused by lithium in various cell lines. *Cell Biol. Internat.* **19:**499–506
31. McConnell, F.M., Goldstein, L. 1988. Intracellular signals and volume regulatory response in skate erythrocytes. *Am. J. Physiol.* **255:**R982–R987
32. Mela, M., Eskelinen, S. 1984. Normal and homogeneous red blood cell populations over a wide range of hyper-iso-hypotonic media. III. Corrected volumes in Coulter Counter measurements. *Acta. Physiol. Scand.* **122:**515–525
33. Mota de Freitas, D., Amari, L., Srinivasan, C., Rong, Q., Ramasamy, R., Abraha, A., Geralses, C.F., Boyd, M.K. 1994. Competition between lithium and magnesium for the phosphate groups in human erythrocyte membrane and ATP: an NMR and fluorescence study. *Biochem.* **33:**4101–4110
34. Musch, M.W., Goldstein, L. 1990. Hypotonicity stimulates phosphatidylcholine hydrolysis and generates diacylglycerol in erythrocytes. *J. Biol. Chem.* **265:**13055–13059
35. Ortiz-Carranza, O., Miller, M.E., Adragna, N.C., Lauf, P.K. 1997*a*. Alkaline pH and internal calcium increase Na and K effluxes in LK sheep red blood cells in Cl-free solutions. *J. Membrane Biol.* **156:**287–295
36. Ortiz-Carranza, O., Adragna, N.C., Carnes, L., Lauf, P.K. 1997*b*. Two operational modes of KCl cotransport in low K sheep red blood cells. *Cell Physiol. Biochem.* **7:**251–263
37. Pappas, A.A., Mullins, R.E., Gadsden, R.H. 1982. Improved one-dimensional thin layer chromatography of phospholipids in amniotic fluid. *Clin. Chem.* **28:**209–211
38. Parker, J.C. 1986. Interactions of lithium and protons with the sodium-proton exchanger of dog red blood cells. *J. Gen. Physiol.* **87:**189–200
39. Parker, J.C. 1993. In defense of cell volume? *Am. J. Physiol.* **265:**C1191–C1200
40. Parker, J.C., McManus, T.J., Starke, L.C., Gitelman, H.J. 1990. Coordinated regulation of Na/H exchange and KCl cotransport in dog red cells. *J. Gen. Physiol.* **96:**1141–1152
41. Plevin, R., Wakelam, M.J. 1992. Rapid desensitization of vasopressin-stimulated phosphatidyl- inositol 4,5-bisphosphate and phosphatidylcholine hydrolysis questions the role of these pathways in sustained diacylglycerol formation in A10 vascular-smooth-muscle cells. *Biochem. J.* **285:**759–766
42. Pollack, S.J., Knowles, M.R., Atack, J.R., Broughton, H.B., Ragan, C.I., Osborne, S.A. 1993. Probing the role of metal ions in the mechanism of inositol monophosphatase by site-directed mutagenesis. *Eur. J. Biochem.* **217:**281–287
43. Ramasamy, R., Freitas, D.M. 1989. Competition between lithium and magnesium for ATP in human erythrocytes. A 31P NMR and optical spectroscopy study. *FEBS Lett.* **244:**223–226
44. Ryu, K.H., Adragna, N.C., Lauf, P.K. 1989. Kinetics of Na-Li exchange in high and low K sheep red blood cells. *Am. J. Physiol.* **257:**C58–C64
45. Sachs, J.R. 1994. Soluble polycations and cationic amphiphiles inhibit volume-sensitive K-Cl cotransport in human red cell ghosts. *Am. J. Physiol.* **266:**C997–C1005
46. Smith, D.K., Lauf, P.K. 1985. Effects of N-ethylmaleimide on ouabain-insensitive cation fluxes in human red cell ghosts. *Biochim. Biophys. Acta* **818:**251–259
47. Somolo, C., Hasson-Voloch, A. 1987. Effect of Li and Ba on the erythrocyte membrane-bound (Na+K) ATPase. *Internat. J. Biochem.* **14:**17–21
48. Sperry, W.M., Brand, F.C. 1955. The determination of total lipids in blood serum. *J. Biol. Chem.* **213:**69–76
49. Srinivasan, M., Begum, N. 1994. Stimulation of protein phosphatase-1 activity by phorbol esters. Evaluation of the regulatory role of protein kinase C in insulin action. *J. Biol. Chem.* **269:**16662–1666–1667
50. Takuwa, Y., Takawa, N., Rasmussen, H. 1986. Carbachol induces a rapid and sustained hydrolysis of polyphosphoinositide in bovine tracheal smooth muscle measurements of the mass of polyphosphoinositides, 1,2-diacyl- glycerol and phosphatidic acid. *J. Biol. Chem.* **261:**14670–14675
51. Tyobeka, E.M., Becker, R.W. 1990. Growth and morphological changes induced by lithium chloride treatment of HL-60 cells. *Cell. Biol. Int. Rep.* **14:**667–679
52. Walter, M., Reinecke, H., Nofer, J.R., Seedorf, U., Assmann, G. 1995. HDL3 stimulates multiple signaling pathways in human skin fibroblasts. *Arterioscler. Thromb. Vasc. Biol.* **15:**1975–1986
53. Zade-Oppen, A.M.M., Lauf, P.K. 1990. Thiol-dependent passive K:Cl transport in sheep red cells. IX. Modulation of pH in the presence and absence of DIDS and the effect of NEM. *J. Membrane Biol.* **118:**143–151